Revista Mexicana de Física **38**, *No. 2 (1992) 262–268*

The influence of the isothermal nitrogen annealing on the generation properties of MOS structures

P. PEYKOV*
Instituto de Ciencias, Universidad Autónoma de Puebla
Apartado postal 1651, 72000 Puebla, Pue. México

M. ACEVES, M. LINARES, W. CALLEJA
Instituto Nacional de Astrofísica, Optica y Electrónica
Apartados Postales 51 y 216, 72000 Puebla, Pue., México

AND

T. DÍAZ
Instituto de Ciencias, Universidad Autónoma de Puebla
Apartado postal 1651, 72000 Puebla, Pue. México

Recibido el 13 de mayo de 1991; aceptado el 9 de octubre de 1991

ABSTRACT. The influence of the isothermal nitrogen annealing on the relaxation time in gettered and non-gettered MOS structures has been investigated. The gettering has been performed on the backside of samples implanted with phosphorus. The annealing time varied from 30 to 120 min. We observed that, in general, isothermal nitrogen annealing results in an increase in the relaxation time. This fact is explained by the shrinkage of oxidation stacking faults. However, for annealing times greater than 90 min it decreases due to the metal impurities diffusion from the ambient. In the case of the gettered samples the initial decrease of relaxation time as a function of annealing time is due to the reversibility of the gettering process. The following slight increase in relaxation time can be explained by the process of shrinkage of the oxidation induced stacking faults which competes with the process of metal impurities diffusion from the ambient.

RESUMEN. Se investiga la influencia del recocido isotérmico con nitrógeno en el tiempo de relajación de estructuras MOS con *gettering* y sin él. El *gettering* fue realizado utilizando implantación de iones en la parte posterior de obleas de silicio. El tiempo de recocido varió de 30 a 120 minutos. En general, se observó que el tiempo de relajación aumenta con el recocido isotérmico utilizando nitrógeno. Este efecto se explica por la reducción de las fallas de apilamiento en el silicio debidas al proceso de oxidación; sin embargo, para tiempos de recocido mayores a 90 minutos, la reducción observada se debe a la difusión de impurezas metálicas provenientes del medio ambiente. En el caso de muestras con *gettering* la reducción inicial del tiempo de relajación, como una función del tiempo de recocido, se debe al carácter reversible del proceso de *gettering*; mientras que el ligero aumento posterior puede explicarse por el proceso de reducción de las fallas inducidas en el silicio por la oxidación, el cual compite con el proceso de difusión de impurezas metálicas contenidas en el medio ambiente.

PACS: 73:40.Qv

---

*University of Sofia, Bulgaria.

1. INTRODUCTION

The role of defects in degrading the electrical performance of semiconductor devices and integrated circuits has been investigated for many years. At the same time, there has been an increasing interest in their elimination. Most of the research was concentrated on the growth and shrinkage of oxidation induced stacking faults (OSF) as well as on the role of metallic impurities. The OSF are electrically active only when decorated with metals.

The elimination of OSF can be obtained by either suppressing the faults nucleation at the beginning of the processing, or implementing process steps which results in the shrinkage of existing stacking faults. For this purpose, different techniques were developed, such as mechanical damage [1], ion implantation [2], phosphorus diffusion [3], HCL [4] or TCE [5] oxidation, deposition of Si_3N_4 films [6] and high temperature annealing [7]. Most of these techniques also cause metal impurity gettering. Because high temperature nitrogen annealing is one of the final process steps in integrated circuits (IC) fabrication, it is important to investigate its effect on the defect kinetics.

The first experimental observations of OSF shrinkage by high-temperature heat-treatments in vacuum were reported by Sanders and Dobson [8], and Ravi [9]. Shrinkage of OSF has been observed also after high-temperature annealing in an inert ambient [4,10–12]. In the last case, the experiments were performed at temperatures ranging from 1050 to 1250°C. However, lower process temperatures are preferable in IC manufacturing.

In the present paper, the influence of nitrogen annealing at 1000°C on the relaxation time, τ_F, of pulsed MOS capacitors is investigated. The relaxation time is proportional to the generation lifetime which in turn is related to the electrically active defects in the silicon.

2. EXPERIMENTAL PROCEDURE

The wafers used in these experiments were phosphorus doped 3–5 ohm-cm (100) oriented silicon crystals grown by the Czochralski method. Two groups of wafers were prepared. The wafers from group I were oxidized at $T = 1000$°C for 40 min in dry O_2, and phosphorus was implanted on the backside through the oxide. The implant dose was 2×10^{15} cm^{-2} and the energy was 120 Kev. The oxide from both sides of the wafers was stripped off. After that the wafers from both groups were oxidized at $T = 1000$°C for $t = 155$ min in dry O_2 to an oxide thickness of 1000 Å.

The wafers from both groups were divided into four subgroups and were annealed in a nitrogen ambient for 30, 60, 90 and 120 min at $T = 1000$°C.

Aluminium dots for MOS structures were deposited through a metal mask. The backside oxide was stripped and Al was deposited to make the backside contact. All wafers were sintered in an N_2/H_2 ambient at $T = 400$°C for 30 min.

The oxide thickness, measured by a Gaertner ellipsometer, was 1030 Å. MOS C–t relaxation measurements were performed at 1 Mhz using a PAR Model 410 capacitance meter. The amplitude of the voltage pulse was 10 volts. From each wafer 30 capacitors were measured.

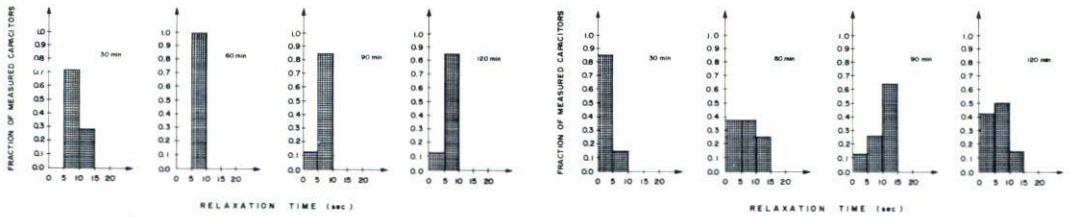

FIGURE 1. Histograms illustrating capacitor frequency versus relaxation time relationship for wafers annealed for different times: (a) samples from group I; (b) samples from group II.

3. EXPERIMENTAL RESULTS

The histograms illustrating the relaxation time frequency for 30, 60, 90 and 120 min annealing time for the wafers from group I and II are shown in Figs. 1(a) and 1(b), respectively. In the case of the samples from group I the highest values of τ_F are for 30 min annealing. Minimum scattering is observed for 60 min annealing.

The relaxation time for the wafers from group II shows minimum scattering and lowest values for 30 min annealing. With the increase of annealing time, a increase of the scattering is observed and the frequency peak for 90 min annealing corresponds to the highest values of τ_F. For 120 min annealing the frequency peak shifts to lower values of τ_F.

The variation of the mean relaxation time value as a function of the annealing time for the samples of both groups is summarized in Fig. 2. The relaxation time of the samples from group I after 30 min annealing, was higher than that of the samples from group II. It decreased after 60 min and after that, it increased slightly after 90 and 120 min annealing. The relaxation time of the samples from group II increased after 30 min to 90 min annealing and after that it decreased, demonstrating a peak after 90 min annealing. For 120 min annealing it coincides with that one of the samples from group I.

4. DISCUSSION

The relatively high relaxation time of the samples from group I for 30 min annealing can be explained as due to the gettering effect of the phosphorus backside implantation. The gettering effect of the heavily doped phosphorus regions in silicon as a result of diffusion [3] or ion implantation [13] is well known. The effectiveness of phosphorus gettering increases with the increase of phosphorus surface concentration [14]. Gettering performed by phosphorus at low concentrations is also effective, and in some cases is preferable [15]. In the case of P backside ion implantation gettering efficiency increases with the implanted dose

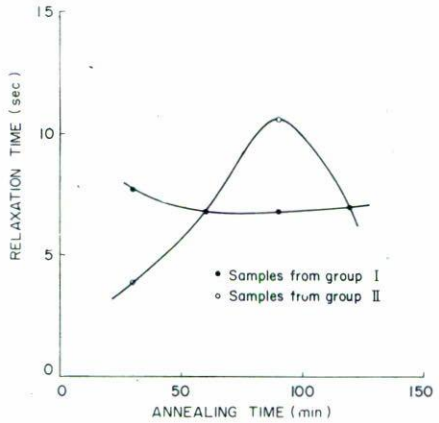

FIGURE 2. Relaxation time versus annealing time.

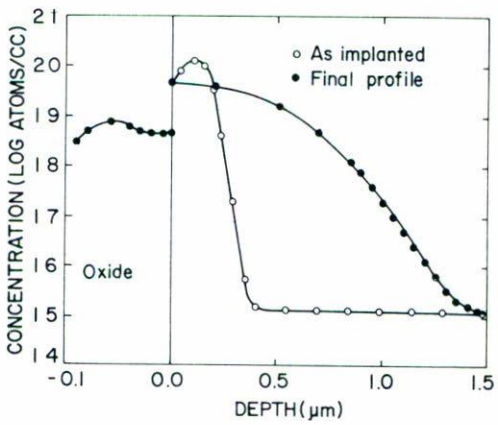

FIGURE 3. Simulated as implanted and final phosphorus profiles at the backside of the gettered wafers.

at least up to 10^{16} ion/cm^2 [16]. In our case the phosphorus implanted dose was not so high. Using "SUPREM II" simulation program [17] we performed a process computer simulation. In Fig. 3, the phosphorus as implanted profile and that obtained after the final oxidation, are shown.

The behavior of the relaxation time of the samples from both groups as a function of the annealing time can be explained by involving the following mechanisms.

1. High concentration of phosphorus or damaged layers serve as a source of self-interstitials. The self-interstitials react with the substitutional heavy metals like Pt or Au by the so called "kick out" mechanism, converting them from low mobility, high solubility substitutionals, to high mobility low solubility interstitial metals which diffuse to the sink [18].

In the case of Ni, Cu and Fe, the generated self-interstitials and impurity metals interact to form silicides in the wafer bulk or perhaps at the surface [19].

2. The gettering process is reversible [14,15], that is the metal impurities can be released at high temperature and can be recaptured at low ones.

3. Because self-diffusion proceeds via interstitial mechanism, OSF shrinkage is also controlled by the motion of interstitials. The activation energy for the OSF shrinkage, 4.9 eV [12], is consistent with the activation energy for silicon self-diffusion, which lies between 4.78 and 5.13 eV [20-22].

It may be assumed that during the annealing step in a neutral ambient, the vacancy and/or self interstitial concentration gradient between the fault and it surroundings [12], together with the bimolecular anhilation mechanism [23], are the driving forces leading to undersaturation of self-interstitials in the bulk surrounding the fault and OSF shrinkage.

According to this model the rate of growth and shrinkage of OSF can be given with the following formula

$$\frac{dL}{dt} = 2\pi a^2 D_I \left[\left(C_I - C_I^B \right) - \left(C_I^S - C_I^B \right) \right], \tag{1}$$

where L is the OSF length, a is the capture radius of silicon self-interstitials by kink, D_I is the diffusion constant of silicon self-interstitials in silicon, C_I is the actual concentration of silicon self-interstitials, C_I^S is the concentration of silicon self-interstitials in equilibrium with the faults, and C_I^B is the thermal equilibrium concentration of silicon self-interstitials in the bulk.

The first term in brackets is related to the absorption of silicon self-interstitials by the faults, *i.e.*, it is related to the OSF growth since $C_I > C_I^B$ under normal oxidation conditions. This term is time dependent. The second term is independent of time and is related to the emission of silicon self-interstitials. It corresponds to OSF shrinkage since $C_I^S > C_I^B$ as a result of the positive change of the free energy in Frank partial dislocation per additional incorporated atom. For the last case, the solution of (1) gives the length of the fault

$$L_0 - L = 2\pi a^2 D_I \left(C_I^S - C_I^B \right) t, \tag{2}$$

where L_0 is the initial OSF length.

4. In the case of nitridation the OSF length increases with oxide thickness up to 700 Å (for dry O_2 oxidation), and decreases after that [24]. Regardless that the mechanisms involved in thermal nitridation process have not been identified yet [25], the following hypotheses exist [24]

a) The shrinkage of preexisting OSF is caused by the emission of self-interstitials from the Frank partial dislocations to the bulk. This emission is enhanced by the undersaturation of silicon self-interstitials near the silicon surface because of silicon cation migration from the silicon-nitride interface to the nitride surface during nitridation.

b) The growth of OSF is caused by the absorption of silicon self interstitials by the Frank partial dislocations. The driving force of this absorption is the supersaturation of

silicon self-interstitials near the surface, which are generated in the film by the reaction of amonia with silicon dioxide and are injected into the bulk of silicon through the nitride-silicon interface.

The inclusion of mechanism (4) in the discussion is questionable, because in our case, the silicon surface is covered with an oxide film. However it is possible to accept that for long annealing times, the silicon surface can be influenced by the nitrogen diffused through the oxide.

5. During annealing metal impurities can diffuse from the ambient into the silicon bulk [26].

6. Ion damaged layers can be annealed [27].

7. When the ion implantation is performed through an oxide layer the knocked-on oxygen atoms produce a significant portion of the ion-implant damage [28].

The initial higher value of τ_F in the case of the samples from group I can be explained by the gettering effect of mechanism (1) and (7). The following decrease of τ_F up to 60 min annealing can be due to mechanism (2) and (6). It was demonstrated that the gettering process is reversible, at least in the case of gold at $T = 1100°C$ and for $t = 10$–15 min [14,15]. In our case the temperature was 1000°C, but the annealing time is much greater. Also, elements like Cu have higher diffusivity than gold. The last hypothesis is confirmed by the results of another experiment. Two wafers were processed the same way as the wafers from group I, but the phosphorus was implanted with a dose of 4×10^{15} cm^{-2} and 150 KeV energy. One of these wafers was annealed for 30 min and the other for 60 min at 1000°C. The mean values of τ_F for these wafers were 18.0 and 11.7 seconds, respectively. The last results indicate that reversible gettering process, when the captured metal impurities are released, is quite probable. Also ion implantation damage can be annealed. With the increase of annealing time to 120 min, relaxation time shows a very slow increase and without an essential change in the scattering of the τ_F values. Because of the lack of a strong tendency in the behavior of τ_F with time, the competing influence of mechanisms (2), (3), (4.*a*), (4.*b*), (5) and (6) is quite possible. In this case the region of high phosphorus concentration can be a source not only of trapped metal impurities, but also of self-interstitials. The flux of these self-interstitials toward the bulk could suppress the effectiveness of mechanisms (3) and (4.*a*).

In the case of the samples of group II, the τ_F value for 30 min annealing is less than the corresponding value for the samples of group I because the lack of gettering. The scattering of τ_F values is not so high. With the increasing of the annealing time to 60 and 90 min the relaxation time increases more than two times. The scattering of the τ_F values increases and the histogram peak for 90 min annealing shifts to the highest τ_F values.

The increase of the relaxation time with the increase of the annealing time up to 90 min can be explained in this case through the dominant role of mechanisms (3) and (4.*a*), *i.e.* the shrinkage of OSF.

The value of τ_F for 120 min annealing shows a decrease and the histogram peak shifts to a lower values of τ_F. These results coincide with the results of Manchanda *et al.* [26] and are explained with the strong influence of mechanism (5), *i.e.* metal impurity diffusion from the ambient during long time annealing.

5. CONCLUSIONS

We have studied the influence of isothermal nitrogen annealing on the relaxation time in gettered and non-gettered MOS structures. We found that, in general, the annealing in nitrogen results in an increase of the relaxation time due to the shrinkage of the oxidation induced stacking faults. However, other different mechanisms such as metal impurities diffusion from the ambient, as well as the reversibility of the gettering process in the case of the gettered samples, can compete with and dominate the first mechanism.

ACKNOWLEDGMENTS

The authors wish to thank Mr. Mauro Landa Vázquez, Microelectronics Technician at INAOE, for his help in preparing the sample used in the experiments and Miss Dulce Polanco for typing the manuscript.

REFERENCES

1. D.I. Pomerantz, *J. Electrochem. Soc.* **119** (1972) 255.
2. S. Prussin, *J. Appl. Phys.* **45** (1974) 1635.
3. G.A. Rozgonyi, P.M. Petroff and M.H. Read, *J. Electrochem. Soc.* **122** (1975) 1725.
4. H. Shiraki, *Jpn. J. Appl. Phys.* **14** (1975) 747.
5. T. Hattori, *J. Electrochem. Soc.* **123** (1976) 945.
6. P.M. Pettrof, G.A. Rozgonyi and T.T. Sheng, *J. Electrochem. Soc.* **123** (1976) 565.
7. K.V. Ravi, *Phil. Mag.* **30** (1974) 1725.
8. I.R. Sanders and P.S. Dobson, *Phil. Mag.* **20** (1969) 881.
9. K.V. Ravi, *Phil. Mag.* **30** (1974) 1081.
10. H. Hashimoto, H. Shibayama, H. Masaki and H. Ishikawa, *J. Electrochem. Soc.* **123** (1976) 1899.
11. Y. Sugita, H. Shimitzu, A. Yoshinaka and T. Aoshina, *J. Vac. Sci. Technol.* **14** (1977) 44.
12. C.L. Clayes, G.J. Declerck and R.J. Von Overstraeten, *Appl. Phys. Lett.* **35** (1979) 797.
13. T.E. Seidel, K.L. Meek and A.G. Cullis, *J. Appl. Phys.* **46** (1975) 600.
14. D. Lecrosnier, J. Paugam, F. Richou, G. Pelous, and F. Beniere, *J. Appl. Phys.* **51** (1980) 1036.
15. L. Baldi, G.F. Cerefolini, G. Ferla and G. Frigerio, *Phys. Stat. Sol. (a)* **48** (1978) 523.
16. K.D. Beyer and T.H. Yeh, *J. Electrochem. Soc.* **129** (1982) 2527.
17. D.A. Antoniadis and R.W. Dutton, *IEEE Trans. El. Dev.*, ED-26 (1979) 490.
18. R. Falster, *Appl. Phys. Lett.* **46** (1985) 737.
19. A. Ourmazd and W. Shroeter, *Appl. Phys. Lett.* **45** (1984) 781.
20. R.F. Peart, *Phys. Stat. Sol.* **15** (1966) 890.
21. R.N. Ghostagore, *Phys. Rev. Lett.* **16** (1966) 890.
22. J.M. Fairfield and R.J. Masters, *J. Appl. Phys.* **38** (1967) 3148.
23. D.A. Antoniadis and I. Moskowitz, *J. Appl. Phys.* **53** (1982) 6788.
24. Y. Hayfuji, K. Kajiware and S. Usui, *J. Appl. Phys.* **53** (1982) 8639.
25. P. Fahey, R.W. Dutton and M. Moslehi, *App. Phys. Lett.* **43** (1983) 683.
26. L. Manchanda, J. Vasi and A.B. Bhattacharyya, *Solid-State Electron.* **23** (1980) 1015.
27. H. Ryssel and I. Ruge, *Ion Implantation*, John Wiley & Sons. Ltd. (1986).
28. C.M. Hsich, J.R. Mathers, H.D. Seidel, K.A. Pickard and C.M. Drum, *Appl. Phys. Lett.* **22** (1973) 238.